

Original Article

## Effects of exosomes derived from platelet-rich plasma on osteogenic differentiation of dental pulp stem cells



Chuzi Mo<sup>1, #</sup>, Zhongjun Liu<sup>1, #</sup>, Yunhe Lin<sup>1</sup>, Nu Er Bi Ya A Bu Du Xi Ku<sup>2</sup>, Siwei Li<sup>1</sup>, Qiao Ruan<sup>1</sup>, Chengxia Liu<sup>1</sup>, Shuaimei Xu<sup>1\*</sup>, Jun Wen<sup>1\*</sup>

<sup>1</sup> Department of Endodontics, Stomatological Hospital, School of Stomatology, Southern Medical University, Guangzhou, Guangdong, 510515, China

<sup>2</sup> Department of Dentistry, The First People's Hospital of Kashgar Prefecture, Kashgar, Xinjiang Uygur Autonomous Region, 844000, China

### Article Info

### Abstract



#### Article history:

**Received:** October 13, 2023

**Accepted:** January 08, 2024

**Published:** February 29, 2024

Use your device to scan and read the article online



Platelet-rich plasma (PRP) can cause osteogenic differentiation of dental pulp stem cells (DPSCs). However, the effect of exosomes derived from PRP (PRP-Exos) on osteogenic differentiation of DPSCs remains unclear. Herein, we evaluated the impact of PRP-Exos on osteogenic differentiation of DPSCs. PRP-Exos were isolated and identified by transmission electron microscopy (TEM) and western blotting (WB). Immunofluorescence staining was performed to evaluate endocytosis of PRP-Exos by DPSCs. Alkaline phosphatase staining, alizarin red staining, western blot and qRT-PCR were carried out to evaluate the DPSCs osteogenic differentiation. The sequencing microRNA (miRNA) was conducted to determine the microRNA profile of PRP-Exos treated and untreated DPSCs. The results showed that endocytosis of PRP-Exos stimulated DPSCs odontogenic differentiation by elevated expression of ALP, DMP-1, OCN, and RUNX2. ALP activity and calcified nodules formation of PRP-Exos treated DPSCs were considerably elevated relative to that of the control group. MicroRNA sequencing revealed that 112 microRNAs considerably varied in PRP-Exos treated DPSCs, of which 84 were elevated and 28 were reduced. Pathway analysis suggested that genes targeted by differentially expressed (DE) miRNAs were contributed to many signaling cascades, such as the Wnt cascade. 65 genes targeted by 30 DE miRNA were contributed to Wnt signaling. Thus, it can be inferred that PRP-Exos could enhance osteogenic differentiation and alter the miRNA expression profile of DPSCs.

**Keywords:** Platelet-rich plasma (PRP); Exosomes; microRNAs; Osteogenic differentiation.

### 1. Introduction

Platelet-rich plasma (PRP) has been shown to improve the osteogenic potential of several stem cells, but the molecular mechanism behind it is yet unknown. Exosomes produced from PRP (PRP-Exos) have been described in several studies to be the principal mechanism by which PRP functions. Dental pulp stem cells (DPSCs), a heterogeneous population of stem cells derived from dental pulp, are an important source of cells for regenerative medicine and tissue engineering applications involving pulp and tooth regeneration. In vital pulp, the number of existing DPSCs is low and gradually loses their differentiating efficiency during in-vitro expansion, thus limiting their application in clinical practices (1). To enhance the future applications of DPSC-based tissue engineering, the DPSCs odonto/osteogenic efficiency needs to be improved. Several factors, such as exosomes, growth factors, pro-inflammatory cytokines (2), mechanical stretch (3), and donor age (4), regulate the proliferative and odonto/osteogenic efficiency of DPSCs. These data provide a si-

gnificant prospect for the reconstruction of the extrinsic microenvironment required to enhance the differentiating efficiency of DPSCs, as well as their application in tissue regeneration.

Platelet-rich plasma (PRP), an autologous whole-blood derivative, has a greater platelet count relative to that in the peripheral blood (5). PRP has been shown to stimulate re-epithelization of chronic cutaneous wounds (6), improve regeneration of bones (7), tendon and ligament repair (8), and chronic femoral osteomyelitis (9). PRP culture medium can trigger osteogenic differentiation of periodontal ligament stem cells (PDLSCs) and DPSCs in vitro (10). PRP treatment has been shown to improve the osteogenic potential of bone marrow-derived mesenchymal stem cells (11). The potential for spontaneous osteogenesis of adipose-derived stem cells has been demonstrated using optimized PRP protocols (12). Furthermore, PRP-containing electrospun polyvinyl-alcohol-chitosan-hydroxyapatite nanofibers can trigger osteogenic differentiation and bone repair in mesenchymal stem cells (13). In a rabbit model

\* Corresponding author.

E-mail address: [xushuaimei@smu.edu.cn](mailto:xushuaimei@smu.edu.cn) (Shuaimei Xu); [Mo13926301033@163.com](mailto:Mo13926301033@163.com) (Jun Wen).

# These authors contributed equally

Doi: <http://dx.doi.org/10.14715/cmb/2024.70.2.32>

with a critical-size radial defect, decellularized bone matrix (PRP-treated) can improve regeneration of bone (14). Activated platelets are anticipated to secrete large amounts of growth factors and cytokines, which are thought to contribute to PRP's main functions, such as increasing chondrocyte proliferation and reducing apoptosis (15, 16). Although PRP offers a lot of potential for osteogenesis, the molecular mechanism behind it is yet unknown. Exosomes produced from PRP have been described in several studies to be the principal mechanism by which PRP functions (17, 18).

Exosomes are tiny vesicles with a diameter ranging between 30 and 150 nm and are believed to transport bioactive lipids, mRNAs, miRNAs, and proteins, thus playing important role in intercellular communication (19). In recent decades, it has been revealed that exosomes are generated from diverse cells and extracellular fluids including stem cells (20), immune cells (21), and bone marrow stem cells (22). Many studies have reported the role of platelet-derived exosomes. In 2004, Janiszewski et al. revealed the isolation of these exosomes and suggested the association between platelet-derived exosomes and the pathophysiology of sepsis (23). Torreggiani et al. isolated exosomes from PRP and were the first to report the function of exosomes (derived from platelet-rich plasma (PRP-Exos)) in regenerating the tissues (24). However, it is unknown whether PRP-Exos influence the osteogenic potential of DPSCs.

This study aimed to identify the contribution of PRP-Exos in proliferation and osteogenic differentiation of DPSCs, and quantify the differentially expressed miRNAs in PRP-Exos treated and untreated DPSCs through RNA-sequencing.

## 2. Materials and methods

### 2.1. Isolation and cell culture of DPSCs

Human dental pulp tissues were taken from clinically healthy permanent teeth that had been removed for orthodontic therapy or an impacted third molar. All of the teeth used in the present study were approved by the Ethical Committee of Stomatological Hospital, Southern Medical University (Approval number: 2021014). To avoid contamination, the teeth were kept in a regular saline solution containing antibiotics. The pulp tissues were minced with a scissor and then digested for 15 minutes at 37 °C with collagenase type I (Sigma Aldrich, St. Louis MO), followed by transferring the Pulp aliquots into 6-well plates and then cultured in an  $\alpha$ -MEM growth medium containing 10% exosome-free FBS, 100 IU/ml penicillin, and 100g/ml streptomycin (Invitrogen/GIBCO). Cells were seeded in two 25 cm<sup>2</sup> plastic tissue culture flasks (BD Biosciences), followed by three days incubation at 37°C in a humidified environment with CO<sub>2</sub> (5%). Red blood cells and other non-adherent cells were discarded on the third day, and a fresh medium was introduced to allow further growth. Passage zero (P0) cells were classified as adherent cells that had grown to 70% confluency. Later paragraphs were renamed to reflect this. For the experiments, cells of 3-5 passages at a 1:3 split ratio were used.

### 2.2. Investigation of DPSC surface markers

Staining of 100  $\mu$ l DPSCs ( $1 \times 10^6$  cells/mL) was carried out by 5  $\mu$ l of each of the following human anti-bodies: FITC anti-CD44, anti-CD45 or anti-CD105 (Beck-

man Coulter), PE anti-CD29, anti-31, anti-CD34 (PharMingen-BD Biosciences) or anti-CD90 (PharMingen-BD Biosciences), followed by incubating the samples at 37 °C for 0.5 hrs. Next, centrifugation was performed for the samples, followed by twice washing with phosphate buffer solution, and then evaluating via flow cytometry (BD, USA).

### 2.3. Preparation of platelet-rich plasma and isolation and identification of exosome

This study recruited 10 healthy volunteers (5 males and 5 females) without any systemic disease, with an average age of 25.1 years. All of the blood specimens used in the present study were approved by the Ethical Committee of Stomatological Hospital, Southern Medical University (Approval number: 2021014). All blood samples were mixed before PRP separation. After collecting venous blood from participants, PRP was separated from erythrocytes and leukocytes using sodium citrate as an anticoagulant, followed by centrifugation for 5 min at 180 $\times$  g. PRP was placed in a clean tube, followed by centrifugation for 15 minutes at 600 $\times$  g. Platelets were pelleted on the tube's bottom. The supernatant plasma and about three-quarters of the platelet-poor plasma layer were discarded, followed by the resuspension of the precipitated platelets in the leftover plasma to yield PRP. PRP was used to raise the platelet count to  $1 \times 10^9$  /mL. Bovine thrombin (1000 U/mL, Sigma-Aldrich, St. Louis, MO, USA) was then added to calcium gluconate (100 mg/mL) at room temperature (for 60 min) to trigger platelet release. After activating the resuspended platelets, the samples were centrifuged for 10, 20, and 30 minutes at 300, 2000, and 10000  $\times$  g, respectively. After each stage of centrifugation, the platelet pellet was collected and discarded. Ultracentrifugation (70 minutes at 100000 $\times$  g) of the supernatant was performed to precipitate exosomes. The exosome pellet was then resuspended in sterile phosphate buffer solution and kept at -80 °C until needed.

A Hitachi H-7650 transmission electron microscopy was used to examine the structure of exosomes isolated from PRP (PRP-Exos). A nanoparticle tracking and NanoSight analysis system (NS300, Malvern Instruments, UK) were used to evaluate the size distribution and concentration of exosomes, and a Bicinchoninic acid Protein Assay Kit was used to evaluate their protein concentrations. Western blotting was performed to evaluate exosome surface markers for CD63 (Abcam Biotechnology, CA), CD41, and CD9 (Invitrogen). As a positive control, platelet lysate (PL) was generated using the procedures reported earlier (Torreggiani et al., 2014).

### 2.4. Fluorescent labeling of exosomes

Pipetting was used to combine 1 $\mu$ l PKH67 (Sigma-Aldrich) with 250  $\mu$ l diluent C, followed by immediate mixing with the exosomes. The staining was terminated by adding an equivalent amount of exosome-free fetal bovine serum after 5 min incubation at  $\sim$  25 °C. Exosomes were extracted and then phosphate buffer solution was used for washing before being resuspended in 100  $\mu$ l exosome-free culture media (100, 000 g for 1 hrs.), followed by adding exosomes (tagged with PKH67) to DPSCs and overnight incubation. The cells were then washed thrice with phosphate buffer solution, followed by cells fixation with 4% paraformaldehyde for 10 min. Next, staining was perfor-

med with 4, 6-diamidino-2-phenylindole (for 5 min). The endocytosis of PRP-Exos by DPSCs was visualized using confocal laser scanning microscopy (Zeiss, Oberkochen, Germany).

## 2.5. Cell viability assay

Cells were seeded into 96-well plates ( $2 \times 10^3$  cells/well) and incubated for 24 hrs. Next, the cells were exposed to 0  $\mu\text{g/mL}$ , and 5 $\mu\text{g/mL}$  PRP-Exos and 15 $\mu\text{g/mL}$  PRP-Exos, followed by adding 20  $\mu\text{L}$  of Cell Counting Kit-8 solution (Dojindo Laboratories, Kumamoto, Japan), and then the incubating the cells for 2 hrs. A microplate reader (BioTek, Winooski, VT, USA) was used to record the optical density of each well at 450 nm wavelength. The results were compared with the results obtained from untreated control for evaluating the viability of the cells. The cells viability was evaluated on days 0, 1, 3, 5, and 7.

## 2.6. Exosome-mediated osteogenic differentiation of DPSCs

Based on various protein concentrations of PRP-Exos cocultured with DPSCs, DPSCs were categorized into 3 groups *i.e.*, 0 $\mu\text{g/mL}$  PRP-Exos, 5 $\mu\text{g/mL}$  PRP-Exos, and 15 $\mu\text{g/mL}$  PRP-Exos. The growth medium was provided with dexamethasone (100 nmol),  $\beta$ -glycerophosphate (10 mmol), and ascorbic acid (50 mg/mL, Sigma, USA) and was used as an osteogenic induction medium. On day 7<sup>th</sup>, an ALP staining kit (86R-1KT; Sigma-Aldrich, Inc) was used to perform the ALP staining, as suggested by the manufacturer, followed by qRT-PCR and western blotting to identify the mRNA associated with osteogenesis and protein expression of ALP, RUNX2, OCN, and DMP-1. On day 21, the calcification nodules were examined by alizarin red staining. Ethanol (70%) was used as a solution for fixation, followed by treating with 2% alizarin red (pH 4.2, Sigma-Aldrich, Inc.). The stained cells were observed

via microscope and the obtained images were then processed via HP Officejet Pro L7580 scanner.

## 2.7. Western blotting analysis

A previously reported protocol was used for western blotting analysis [58]. Exosomal protein was extracted via an Exosomal Protein Extract Buffer (EZBioscience, Roseville, USA). The protein of DPSCs was extracted (exposed to 0 $\mu\text{g/mL}$  PRP-Exos, 5 $\mu\text{g/mL}$  PRP-Exos, and 15 $\mu\text{g/mL}$  PRP-Exos) on day 7 via RIPA lysis buffer (Solarbio, Beijing, China). Bicinchoninic acid Protein Assay Kit (Pierce, Rockford, IL, USA) was used to determine the total concentration of the proteins. Next, the loading buffer was added with the extracted protein (30  $\mu\text{g}$ ), followed by denaturation of the protein in boiling water (for 5 min). Sodium dodecyl sulfate polyacrylamide gel electrophoresis (10% w/v) was used for the protein separation. Then the protein was transferred to the polyvinylidene difluoride membrane. For blockage purposes, Bovine serum albumin (5% (w/v), Sangon Biotech, Shanghai) was used for 60 min at  $\sim 25^\circ\text{C}$ , followed by membrane probing with ALP (1:500 dilution, Abcam), RUNX2 (1:1000 dilution, Cell Signaling Technology), OCN (1:1000 dilution, Abcam), GAPDH (1:8000 dilution, Proteintech) and DMP-1 (1:1000 dilution, Bioss) for 24 hrs at  $4^\circ\text{C}$ . Post washing with Tris-buffered saline with Tween-20 (TBST), the membranes were incubated with the secondary antibodies (Cell Signaling Technology) conjugated with horseradish peroxidase (HRP) (1:3000 dilution) at  $\sim 25^\circ\text{C}$  for 60 min. TBST was used to wash unbound antibodies. The ECL imaging kit (Thermo Fisher Scientific) was used to generate the chemiluminescent signal. GAPDH was used as an internal control.

## 2.8. Real-time quantitative PCR

RNA extraction kit (Qiagen, China) was used for total

**Table 1.** Primer pairs used in the qRT-PCR.

Name	Primers(5'-3')
ALP-F	GGACATGCAGTACGAGCTGA
ALP-R	GCAGTGAAGGGCTTCTTGTC
RUNX2-F	TGGTTACTGTCATGGCGGGTA
RUNX2-R	TCTCAGATCGTTGAACCTTGCTA
OCN-F	CTACCCGGATCCCCTGGAG
OCN-R	GCCGTAGAAGCGCCGATAG
DMP1-F	CATTTGGCTCAGGCACCAAC
DMP1-R	GCTCCTGGAGAAGCCACC
GAPDH-F	GAGTCAACGGATTTGGTCGT
GAPDH-R	GACAAGCTTCCCCTTCTCAG
hsa-miR-1538-RT	GTCGTATCCAGTGCAGGGTCCGAGGTATTTCGCACTGGATACGACAGGAAC
hsa-miR-1538-F	CGGCCCGGGCTGCTGCTGT
hsa-miR-3620-5p-RT	GTCGTATCCAGTGCAGGGTCCGAGGTATTTCGCACTGGATACGACGGCCCA
hsa-miR-3620-5p-F	GTGGGCTGGGCTGGGCTG
hsa-miR-1909-3p-RT	GTCGTATCCAGTGCAGGGTCCGAGGTATTTCGCACTGGATACGACCGGTGA
hsa-miR-1909-3p-F	CGCAGGGGCCGGGTGCTC
hsa-miR-4651-RT	GTCGTATCCAGTGCAGGGTCCGAGGTATTTCGCACTGGATACGACGCCCGA
hsa-miR-4651-F	CGGGGTGGGTGAGGTC
miR-Universe-R	GTGCAGGGTCCGAGGT
hsa-U6-F	CTCGCTTCGGCAGCACA
hsa-U6-R	AACGCTTCACGAATTTGCGT

F: forward primer. R: reverse primer

RNA extraction from cells. An RT-PCR system (Promega, USA) was employed to synthesize cDNA from total RNA (2 $\mu$ g), followed by the qRT-PCR via SYBR-Green PCR kit (Qiagen, China) on a LightCycler 480 (Roche, USA), as suggested by the manufacturer. The results were obtained from three independent experiments. The comparative Ct ( $\Delta\Delta$ Ct) technique was used to evaluate the relative expression of microRNA. Table 1 enlists the sequences of the primers.

## 2.9. MicroRNA sequencing

The DPSCs incubated for 7 days in an osteogenic induction medium supplemented with 0 or 15  $\mu$ g/mL PRP-exos were used for microRNA sequencing. Denaturing PAGE (15%) was used to obtain microRNAs comprising of 18 to 30 nucleotides (nt) from total RNA (100  $\mu$ g isolated from exosomes). Post PCR amplification, the product was purified and then were submitted for sequencing through Illumina Hi-Seq 2000. Library preparation and micro-RNA sequencing were obtained from RiboBio Ltd. (Guangzhou, China), followed by analyzing differentially expressed miRNAs with 2 fold variation in expression ( $p < 0.05$ ). Four accessible bioinformatics tools (TargetScan, miRTarBase, miRDB, and miRWalk data-bases) were employed to evaluate Predicted microRNA target genes. Kyoto Encyclopedia of Genes and Genomes (<http://www.genome.jp/kegg/pathway.html>) Pathway analysis was carried out to determine cascades linked with the predicted microRNA target genes.

## 2.10. Statistical analysis

All experimental procedures were repeated three times. The obtained results were represented as the mean  $\pm$  S.D. SPSS 20.0 (IBM Corp., Armonk, NY, USA) was employed for analyzing statistical data, followed by constructing bar charts via GraphPad Prism version 7.0 (San Diego, CA, USA). Next, two-tailed Student's t-test or one-way ANOVA were used for comparing results. P-value  $< 0.05$  was regarded as statistically significant.

## 3. Results

### 3.1. Isolation and identification of DPSCs

Flow cytometry was used to confirm the identity of the DPSCs used in this investigation. The cells were shown to be positive for MSC markers *i.e.*, CD29, CD44, CD90, and CD105 while negative for the hematopoietic stem cell markers *i.e.*, CD31, CD34, and CD45. The obtained results showed the successful isolation and culturing of DPSCs, as depicted in Fig. 1A-G.

### 3.2. Characterization of PRP-Exos

Transmission electron microscopy, nanoparticle tracking and NanoSight analysis technology, and western blotting were used for the characterization of PRP-Exos. Nanoparticle tracking and NanoSight analysis showed that 98.3% of PRP-Exos particles were  $114.7 \pm 70.5$  nm in diameter (Fig. 2A). Transmission electron microscopy indicated a round-shaped structure of PRP-Exos, as depicted in Fig. 2B. While the results obtained from Western blotting suggested that exosomal markers including CD63, CD9, and CD41, were found to be expressed in PRP-, as depicted in Fig. 2C. The obtained results revealed that the nanoparticles derived from PRP were PRP-Exos.

### 3.3. Endocytosis of PRP-Exos by DPSCs triggered osteogenic differentiation

To confirm whether DPSCs might take up PRP-Exos, the labeling of extracted PRP-Exos was carried out with PKH67, followed by incubating DPSC cultures with the labeled exosomes at 37  $^{\circ}$ C. After 24 hrs, PRP-Exos (labeled with PKH67) were taken up into the cytoplasm by DPSCs, as depicted in Fig. 3.

We then assessed the effect of PRP-Exos on DPSCs viability using the Cell Counting Kit-8 assay and found that DPSCs growth was not affected by PRP-Exos (Fig. 4A). Next, we identified whether the endocytosis of PRP-Exos stimulated osteogenic differentiation of DPSCs after one week with the induction of the osteogenic medium, PRP-Exos treated groups showed increased ALP staining activity in a dose-dependent manner (Fig. 4B). Increased

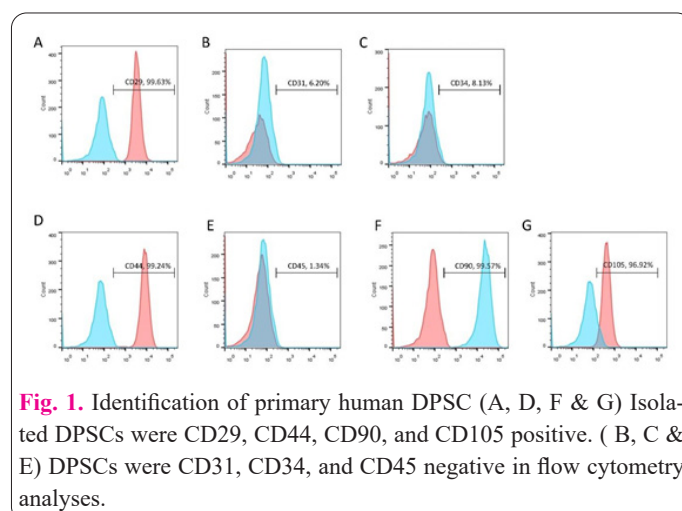


**Fig. 1.** Identification of primary human DPSC (A, D, F & G) Isolated DPSCs were CD29, CD44, CD90, and CD105 positive. (B, C & E) DPSCs were CD31, CD34, and CD45 negative in flow cytometry analyses.

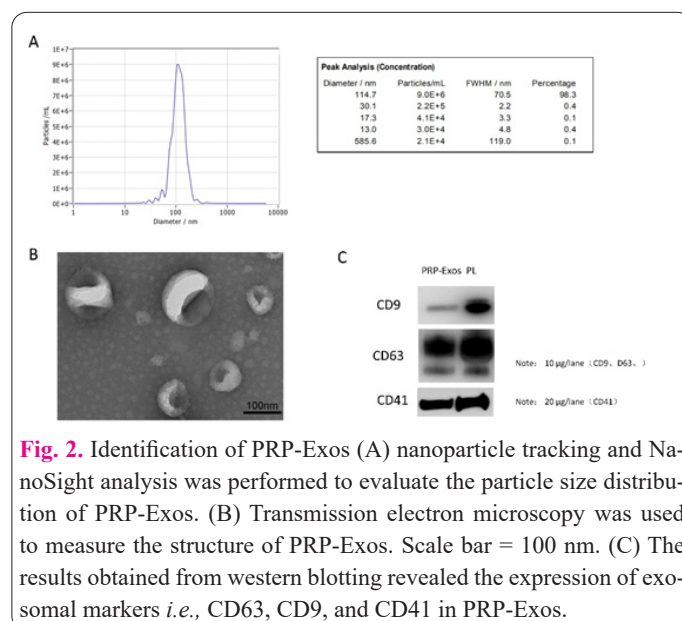


**Fig. 2.** Identification of PRP-Exos (A) nanoparticle tracking and NanoSight analysis was performed to evaluate the particle size distribution of PRP-Exos. (B) Transmission electron microscopy was used to measure the structure of PRP-Exos. Scale bar = 100 nm. (C) The results obtained from western blotting revealed the expression of exosomal markers *i.e.*, CD63, CD9, and CD41 in PRP-Exos.

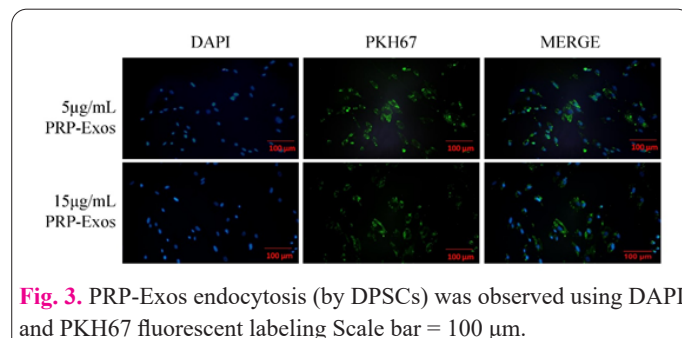


**Fig. 3.** PRP-Exos endocytosis (by DPSCs) was observed using DAPI and PKH67 fluorescent labeling Scale bar = 100  $\mu$ m.

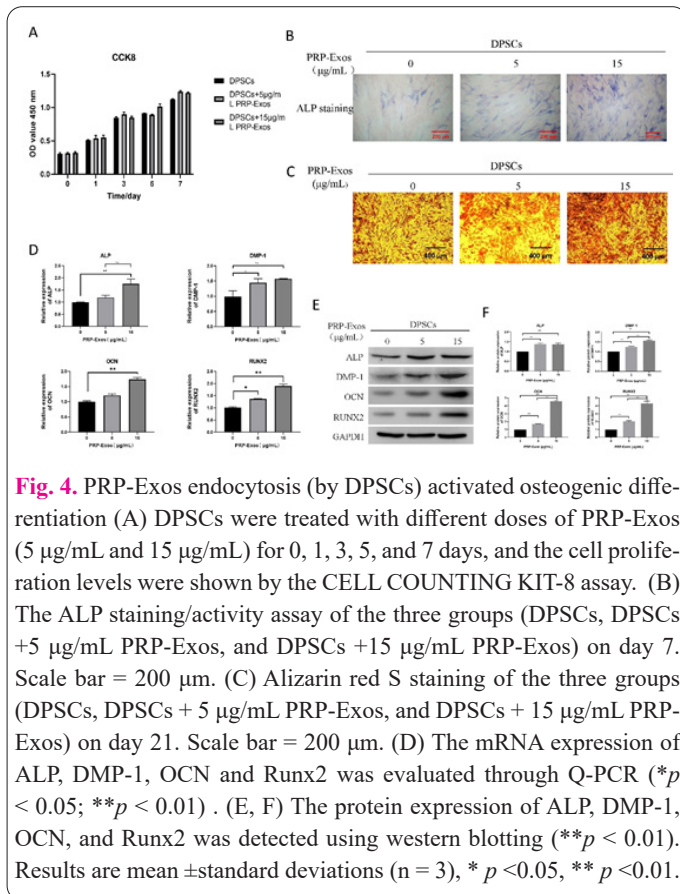


**Fig. 4.** PRP-Exos endocytosis (by DPSCs) activated osteogenic differentiation (A) DPSCs were treated with different doses of PRP-Exos (5 µg/mL and 15 µg/mL) for 0, 1, 3, 5, and 7 days, and the cell proliferation levels were shown by the CELL COUNTING KIT-8 assay. (B) The ALP staining/activity assay of the three groups (DPSCs, DPSCs +5 µg/mL PRP-Exos, and DPSCs +15 µg/mL PRP-Exos) on day 7. Scale bar = 200 µm. (C) Alizarin red S staining of the three groups (DPSCs, DPSCs + 5 µg/mL PRP-Exos, and DPSCs + 15 µg/mL PRP-Exos) on day 21. Scale bar = 200 µm. (D) The mRNA expression of ALP, DMP-1, OCN and Runx2 was evaluated through Q-PCR (\* $p < 0.05$ ; \*\* $p < 0.01$ ). (E, F) The protein expression of ALP, DMP-1, OCN, and Runx2 was detected using western blotting (\*\* $p < 0.01$ ). Results are mean  $\pm$  standard deviations ( $n = 3$ ), \* $p < 0.05$ , \*\* $p < 0.01$ .

calcified nodules in PRP-Exos treated groups after 3 weeks were also observed by alizarin red staining (Fig. 4C). The results of RT-PCR showed that after the osteogenic medium and 15µg/mL PRP-Exos treatment on day 7, the expression of ALP, OCN, and DMP-1mRNA increased. However, the expression of gene Runx2 in the PRP-Exos groups showed no significant difference with a slight up-regulation (Fig. 4D). The results obtained from western blotting revealed that PRP-Exos treatment (one week) considerably elevated translational level of ALP, Runx2, OCN, and DMP-1; the expression level of Runx2, OCN, and DMP-1 in the 15µg/mL PRP-Exos group was elevated relative to that in the 5µg/mL PRP-Exos group, as shown in Fig. 4E&F.

### 3.4. MicroRNA profiles of PRP-Exos treated DPSCs

Exosomes transmitted microRNAs between cells. In recipient cells, microRNAs (present in exosomes) might regulate gene expression at the post-transcriptional level. Hence, it has been postulated that DPSCs might use the underlined process to enhance osteogenic differentiation. For extensive understanding, the microRNA profiles of 0µg/mL (control group) and 15µg/mL PRP-Exos treated DPSCs were analyzed via Ion Torrent/ MiSeq sequencing. The obtained data revealed that the level of microRNA in 15µg/m PRP-Exos treated DPSCs considerably varied relative to that in the control group. In PRP-Exos treated DPSCs under osteogenic conditions, 112 microRNAs significantly differed, with 84 microRNAs elevating and 28 microRNAs reducing, as shown in Fig. 5A. Four accessible bioinformatics tools were used to examine genes targeted by differentially expressed miRNAs. Kyoto Encyclopedia of Genes and Genomes pathway analysis suggested the involvement of targeted genes in many signaling cascades, such as the Wnt signaling cascade. 30

differentially expressed miRNAs target 65 genes in Wnt signaling (Fig. 5B&C). The qRT-PCR was carried out to verify the top 4 miRNAs with the largest number of target genes. The results showed that miR-1909-3p, miR-4651, miR-1538 and miR-3620-5p levels in PRP-Exos treated DPSCs increased, which was consistent with the microRNA sequencing (Fig. 6).

## 4. Discussion

PRP also known as autologous platelets, is comprised of four to five times more platelets relative to unprocessed blood plasma. PRP has been shown to stimulate osteogenesis not only in DPSCs, but also in periodontal ligament stem cells and mesenchymal stem cells produced from the umbilical cord, adipose tissue, and bone marrow in vitro (25). PRP can boost stem cell attachment, proliferation, migration, and differentiation into target tissue due to its content material, which includes epidermal growth factor,

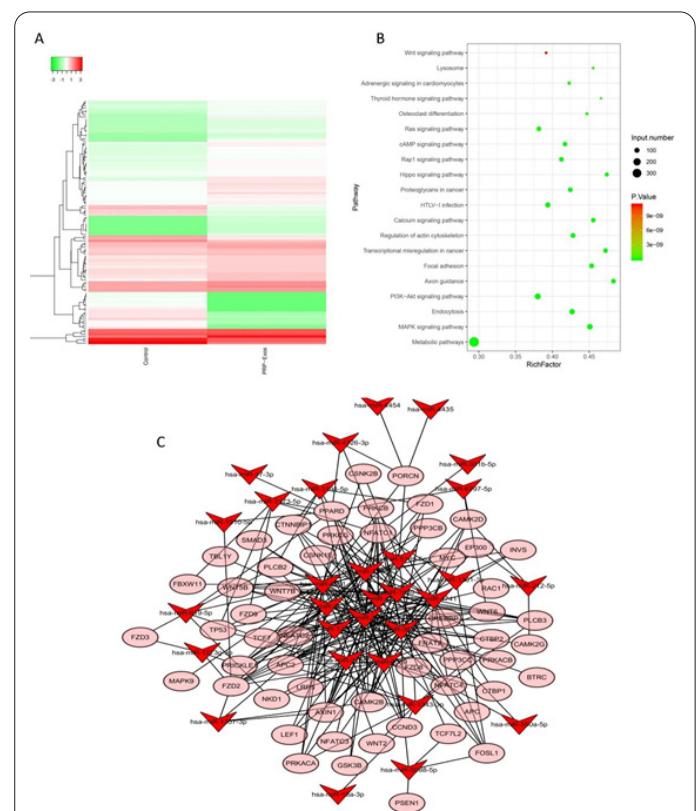


**Fig. 5.** microRNA profiles of PRP-Exos treated and untreated DPSCs via microRNA sequencing (A) The level of microRNA (112) was considerably varied in DPSCs (treated with PRP-Exos) relative to that in the control group, with 84 elevated and 28 reduced. (B) mRNA-microRNA network revealed that 65 genes (in Wnt signaling) were targeted by 30 differentially expressed miRNAs. (C) The analysis of cascades revealed that targeted genes were found to be involved in many signaling cascades, such as Wnt signaling cascade.

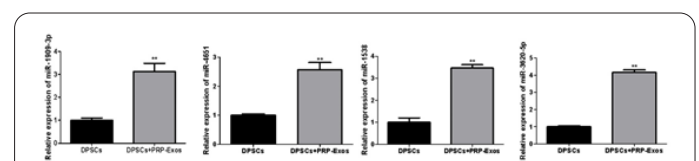


**Fig. 6.** qRT-PCR verification of microRNA-seq results miR-1909-3p and miR-4651, miR-1538 and miR-3620-5p levels in PRP-Exos treated DPSCs increased by qRT-PCR analysis, which showed consistency with the results obtained from the microRNA sequencing. Results are mean  $\pm$  standard deviations ( $n = 3$ ), \*\* $p < 0.01$ .

fibroblastic growth factor, transforming growth factor, and platelet-derived growth factor (26, 27). As a result, PRP is commonly employed in guided tissue/bone regeneration. Furthermore, DPSCs with PRP demonstrated osteogenic potential around dental implants *in vivo* (28). However, to the best of our knowledge, the effects of PRP-Exos on the osteogenic development of DPSCs have never been investigated. In regenerative endodontic treatment, exosomes can be employed as biomimetic tools to stimulate odontoblast-specific differentiation of DPSCs (29). We were able to successfully separate exosomes from platelet-rich plasma (PRP), which is crucial for DPSC osteogenic development. PRP-Exos endocytosis induced osteogenic differentiation in DPSCs by increasing the expression of alkaline phosphatase (ALP), dentin matrix acidic phosphoprotein 1 (DMP1), osteocalcin (OCN) and runt related transcription factor 2 (RUNX2). The mineralization augmentation was further demonstrated by ALP and alizarin red staining, which is compatible with PRP's effect on DPSC differentiation (30). Exosomes from various cell types have also been shown to trigger lineage-specific differentiation of stem cells in previous research. Exosomes generated from DPSCs can drive the differentiation of bone marrow mesenchymal stem cells towards an odontogenic lineage (29). Likewise, instructive factors in osteoblast-derived exosomes enhanced MSC osteogenic differentiation, whereas adipocyte-derived exosomes stimulated MSC adipogenic differentiation (31).

Exosomes considerably mediate intercellular communication by transporting cell-specific biological molecules including mRNA, microRNA, and protein (31). Exosomal microRNAs interact with their target mRNAs via base pairing to the 3'-UTR that results in the translational repression of the mRNA in recipient cells, thus negatively regulate gene expression (32). Exosomal microRNAs are critical in the differentiation of stem cells (33) but the function of microRNAs contained in PRP-Exos has yet to be determined. Herein, MicroRNA sequencing was used to evaluate the microRNA expression profiles of DPSCs treated with PRP-Exos. The results showed that microRNA levels in DPSCs treated with PRP-Exos were considerably varied relative to that in untreated DPSCs. microRNAs (112) considerably varied with 84 microRNAs increased and 24 microRNAs decreased. Among these, some miRNAs considerably contribute to the differentiation of stem cells. For example, overexpression of miR-3960 promotes BMP2-induced osteoblastogenesis of ST2 stromal cells (34). miR-1301-3p can enhance osteogenic differentiation of human mesenchymal stem cells via PROX1 (35). miR-193a-3p has a crucial role in the transduction of biophysical signals from the substrate to regulate the osteogenic lineage specification of mesenchymal stem cells (36). miR-485-5p, miR-206, miR-17-3p and miR-144-3p could suppresses osteogenic differentiation of mesenchymal stem cells (37-39). Decreased expression of miR-451a could promote the formation of bone during the development of osteoporosis in mice (40). Moreover, miR-1, miR-206, miR-133a, miR-133b can enhance osteogenic differentiation of primary mesenchymal progenitor cells (41).

In the current study, four freely accessible bioinformatics tools were employed to predict genes targeted by differentially expressed miRNAs. Genes targeted by differentially expressed miRNAs were contributed in numerous signaling cascades, such as the Wnt signaling cascade,

according to pathway analysis. Wnt signaling has been found to have a key role in tooth formation and osteogenic differentiation (42). Moreover, Wnt signaling is widely associated with miRNAs and exosomes. For instance, exosomal miR-130a-3p mediates miR-130a-3p/Wnt/ $\beta$ -catenin axis in order to regulate osteogenic differentiation of stem cells (derived from human adipose) (43). Exosomes derived from mineralizing osteoblasts moderately activate variation in the expression of miRNA in recipient bone marrow stromal cells via exosomal miRNA transfer, and this variation tend to stimulate the Wnt signaling cascade, leading to osteogenic differentiation of recipient cells (44). Exosomes (from myoblasts *i.e.*, C2C12) may enhance differentiation of pre-osteoblasts (MC3T3-E1) to osteoblasts by delivering miR-27a-3p, thus activating the Wnt/ $\beta$ -catenin pathway (45). miR-19b enriched in BMSC-derived exosomes promote healing of bone fracture *in vivo* via Wnt/ $\beta$ -catenin signaling cascade (46). There is a need to validate whether Wnt signaling was triggered by PRP-exosomal microRNAs to promote DPSCs osteogenic differentiation.

## 5. Conclusions

This study proved that PRP-Exos are inducers of DPSCs osteogenic differentiation. MicroRNAs expression profile of PRP-Exos treated DPSCs significantly changed compared to that of DPSCs without PRP-Exos treatment. Genes targeted by differentially expressed miRNAs contributed to numerous signaling cascades, such as the Wnt signaling cascade. Further studies are needed to authenticate the regulatory mechanism and clinical applications of PRP-Exos on DPSCs osteogenic differentiation.

## Competing interests

The authors have no relevant financial or non-financial interests to disclose.

## Availability of data and materials

The data that support the findings of this study are available from the corresponding author upon reasonable request.

## Ethics approval

This study was performed in line with the principles of the Declaration of Helsinki. Approval was granted by the Research Ethics Committee of Somatological Hospital, Southern Medical University (Approval number: 2021014).

## Funding

This work was supported by the Scientific Research Cultivation Project of Stomatological Hospital, Southern Medical University (Grant No. PY2019010, No. PY2021018 and No. PY2022028) and Guangzhou Municipal Science and Technology Plan Project (Grant No. 202201011515).

## Author contributions

Shuaimi Xu and Jun Wen designed the study, Chuzi Mo and Zhongjun Liu wrote the manuscript, Yunhe Lin and Nu Er Bi Ya A Bu Du Xi Ku collected and analyzed data, Siwei Li, Qiao Ruan and Chengxia Liu revised the manuscript, Chuzi Mo and Zhongjun Liu made equal contributions in this work. All authors read and approved the final submitted manuscript.

## References

1. Yu J, He H, Tang C, et al. Differentiation potential of STRO-1+ dental pulp stem cells changes during cell passaging. *BMC Cell Biol.* 2010; 11:32. doi:10.1186/1471-2121-11-32
2. Kim SG, Zhou J, Solomon C, et al. Effects of growth factors on dental stem/progenitor cells. *Dent. Clin. North Am.* 2012; 56(3):563-575. doi:10.1016/j.cden.2012.05.001
3. Hata M, Naruse K, Ozawa S, et al. Mechanical stretch increases the proliferation while inhibiting the osteogenic differentiation in dental pulp stem cells. *Tissue Eng. Part A.* 2013; 19(5-6):625-633. doi:10.1089/ten.tea.2012.0099
4. Ma D, Ma Z, Zhang X, et al. Effect of age and extrinsic microenvironment on the proliferation and osteogenic differentiation of rat dental pulp stem cells in vitro. *J. Endod.* 2009; 35(11):1546-1553. doi:10.1016/j.joen.2009.07.016
5. Yuan T, Guo S-C, Han P, Zhang C-Q, Zeng B-F. Applications of leukocyte- and platelet-rich plasma (L-PRP) in trauma surgery. *Curr. Pharm. Biotechnol.* 2012; 13(7):1173-1184.
6. Guo S-C, Tao S-C, Yin W-J, Qi X, Yuan T, Zhang C-Q. Exosomes derived from platelet-rich plasma promote the re-epithelization of chronic cutaneous wounds via activation of YAP in a diabetic rat model. *Theranostics.* 2017; 7(1):81-96. doi:10.7150/thno.16803
7. Kim Y-H, Furuya H, Tabata Y. Enhancement of bone regeneration by dual release of a macrophage recruitment agent and platelet-rich plasma from gelatin hydrogels. *Biomaterials.* 2014; 35(1):214-224. doi:10.1016/j.biomaterials.2013.09.103
8. Yuan T, Zhang C-Q, Wang JHC. Augmenting tendon and ligament repair with platelet-rich plasma (PRP). *Muscles, ligaments and tendons journal.* 2013; 3(3):139-149.
9. Yuan T, Zhang C, Zeng B. Treatment of chronic femoral osteomyelitis with platelet-rich plasma (PRP): a case report. *Transfusion and apheresis science : official journal of the World Apheresis Association : official journal of the European Society for Haemapheresis.* 2008; 38(2):167-173. doi:10.1016/j.transci.2008.01.006
10. Otero L, Carrillo N, Calvo-Guirado JL, Villamil J, Delgado-Ruiz RA. Osteogenic potential of platelet-rich plasma in dental stem-cell cultures. *The British journal of oral & maxillofacial surgery.* 2017; 55(7):697-702. doi:10.1016/j.bjoms.2017.05.005
11. Chen L, Yang X, Huang G, et al. Platelet-rich plasma promotes healing of osteoporotic fractures. *Orthopedics.* 2013; 36(6):e687-e694. doi:10.3928/01477447-20130523-10
12. Gersch RP, Glahn J, Tecce MG, Wilson AJ, Percec I. Platelet Rich Plasma Augments Adipose-Derived Stem Cell Growth and Differentiation. *Aesthetic Surgery Journal.* 2017; 37(6):723-729. doi:10.1093/asj/sjw235
13. Abazari MF, Nejati F, Nasiri N, et al. Platelet-rich plasma incorporated electrospun PVA-chitosan-HA nanofibers accelerates osteogenic differentiation and bone reconstruction. *Gene.* 2019; 720:144096. doi:10.1016/j.gene.2019.144096
14. Leng Y, Ren G, Cui Y, et al. Platelet-rich plasma-enhanced osseointegration of decellularized bone matrix in critical-size radial defects in rabbits. *Annals of translational medicine.* 2020; 8(5):198. doi:10.21037/atm.2020.01.53
15. Yin WJ, Xu HT, Sheng JG, et al. Advantages of Pure Platelet-Rich Plasma Compared with Leukocyte- and Platelet-Rich Plasma in Treating Rabbit Knee Osteoarthritis. *Med Sci Monit.* 2016; 22:1280-1290. doi:10.12659/msm.898218
16. Forogh B, Mianehsaz E, Shoaee S, Ahadi T, Raissi GR, Sajadi S. Effect of single injection of platelet-rich plasma in comparison with corticosteroid on knee osteoarthritis: a double-blind randomized clinical trial. *The Journal of sports medicine and physical fitness.* 2016; 56(7-8):901-908.
17. Tao SC, Yuan T, Rui BY, Zhu ZZ, Guo SC, Zhang CQ. Exosomes derived from human platelet-rich plasma prevent apoptosis induced by glucocorticoid-associated endoplasmic reticulum stress in rat osteonecrosis of the femoral head via the Akt/Bad/Bcl-2 signal pathway. *Theranostics.* 2017; 7(3):733-750. doi:10.7150/thno.17450
18. Liu X, Wang L, Ma C, Wang G, Zhang Y, Sun S. Exosomes derived from platelet-rich plasma present a novel potential in alleviating knee osteoarthritis by promoting proliferation and inhibiting apoptosis of chondrocyte via Wnt/ $\beta$ -catenin signaling pathway. *J Orthop Surg Res.* 2019; 14(1):470. doi:10.1186/s13018-019-1529-7
19. Beit-Yannai E, Tabak S, Stamer WD. Physical exosome:exosome interactions. *J. Cell. Mol. Med.* 2018; 22(3):2001-6. doi:10.1111/jcmm.13479
20. Burke J, Kolhe R, Hunter M, Isales C, Hamrick M, Fulzele S. Stem Cell-Derived Exosomes: A Potential Alternative Therapeutic Agent in Orthopaedics. *Stem Cells Int.* 2016; 2016:5802529. doi:10.1155/2016/5802529
21. McCoy-Simandle K, Hanna SJ, Cox D. Exosomes and nanotubes: Control of immune cell communication. *Int. J. Biochem. Cell Biol.* 2016; 71:44-54. doi:10.1016/j.biocel.2015.12.006
22. Mao G, Zhang Z, Huang Z, et al. MicroRNA-92a-3p regulates the expression of cartilage-specific genes by directly targeting histone deacetylase 2 in chondrogenesis and degradation. *Osteoarthritis Cartilage.* 2017; 25(4):521-532. doi:10.1016/j.joca.2016.11.006
23. Janiszewski M, Do Carmo AO, Pedro MA, Silva E, Knobel E, Laurindo FR. Platelet-derived exosomes of septic individuals possess proapoptotic NAD(P)H oxidase activity: A novel vascular redox pathway. *Crit. Care Med.* 2004; 32(3):818-825. doi:10.1097/01.ccm.0000114829.17746.19
24. Torreggiani E, Perut F, Roncuzzi L, Zini N, Baglio SR, Baldini N. Exosomes: novel effectors of human platelet lysate activity. *Eur. Cell. Mater.* 2014; 28:137-51; discussion 51. doi:10.22203/ecm.v028a11
25. Qi Y, Niu L, Zhao T, et al. Combining mesenchymal stem cell sheets with platelet-rich plasma gel/calcium phosphate particles: a novel strategy to promote bone regeneration. *Stem Cell Res Ther.* 2015; 6:256. doi:10.1186/s13287-015-0256-1
26. Enderami SE, Mortazavi Y, Soleimani M, Nadri S, Biglari A, Mansour RN. Generation of Insulin-Producing Cells From Human-Induced Pluripotent Stem Cells Using a Stepwise Differentiation Protocol Optimized With Platelet-Rich Plasma. *J. Cell. Physiol.* 2017; 232(10):2878-2886. doi:10.1002/jcp.25721
27. Alves R, Grimalt R. A Review of Platelet-Rich Plasma: History, Biology, Mechanism of Action, and Classification. *Skin Appendage Disord.* 2018; 4(1):18-24. doi:10.1159/000477353
28. Irastorza I, Luzuriaga J, Martinez-Conde R, Ibarretxe G, Unda F. Adhesion, integration and osteogenesis of human dental pulp stem cells on biomimetic implant surfaces combined with plasma derived products. *Eur. Cell. Mater.* 2019; 38:201-214. doi:10.22203/eCM.v038a14
29. Huang CC, Narayanan R, Alapati S, Ravindran S. Exosomes as biomimetic tools for stem cell differentiation: Applications in dental pulp tissue regeneration. *Biomaterials.* 2016; 111:103-15. doi:10.1016/j.biomaterials.2016.09.029
30. Otero L, Carrillo N, Calvo-Guirado JL, Villamil J, Delgado-Ruiz RA. Osteogenic potential of platelet-rich plasma in dental stem-cell cultures. *Br. J. Oral Maxillofac. Surg.* 2017; 55(7):697-702. doi:10.1016/j.bjoms.2017.05.005
31. Narayanan K, Kumar S, Padmanabhan P, Gulyas B, Wan ACA, Rajendran VM. Lineage-specific exosomes could override extracellular matrix mediated human mesenchymal stem cell differentiation. *Biomaterials.* 2018; 182:312-322. doi:10.1016/j.biomaterials.2018.08.027

32. Bhome R, Del Vecchio F, Lee GH, et al. Exosomal microRNAs (exomiRs): Small molecules with a big role in cancer. *Cancer Lett.* 2018; 420:228-235. doi:10.1016/j.canlet.2018.02.002
33. Fang S, Xu C, Zhang Y, et al. Umbilical Cord-Derived Mesenchymal Stem Cell-Derived Exosomal MicroRNAs Suppress Myofibroblast Differentiation by Inhibiting the Transforming Growth Factor- $\beta$ /SMAD2 Pathway During Wound Healing. *Stem Cells Transl Med.* 2016; 5(10):1425-1439. doi:10.5966/sctm.2015-0367
34. Hu R, Liu W, Li H, et al. A Runx2/miR-3960/miR-2861 regulatory feedback loop during mouse osteoblast differentiation. *J. Biol. Chem.* 2011; 286(14):12328-12339. doi:10.1074/jbc.M110.176099
35. Weng W, Di S, Xing S, et al. Long non-coding RNA DANCR modulates osteogenic differentiation by regulating the miR-1301-3p/PROX1 axis. *Mol. Cell. Biochem.* 2021; 476(6):2503-2512. doi:10.1007/s11010-021-04074-9
36. Lv Y, Huang Y, Xu M, et al. The miR-193a-3p-MAP3k3 Signaling Axis Regulates Substrate Topography-Induced Osteogenesis of Bone Marrow Stem Cells. *Adv Sci (Weinh).* 2020; 7(1):1901412. doi:10.1002/advs.201901412
37. Li N, Liu L, Liu Y, Luo S, Song Y, Fang B. miR-144-3p Suppresses Osteogenic Differentiation of BMSCs from Patients with Aplastic Anemia through Repression of TET2. *Mol Ther Nucleic Acids.* 2020; 19:619-626. doi:10.1016/j.omtn.2019.12.017
38. Chen N, Wu D, Li H, Liu Y, Yang H. MiR-17-3p inhibits osteoblast differentiation by downregulating Sox6 expression. *FEBS Open Bio.* 2020; 10(11):2499-2506. doi:10.1002/2211-5463.12979
39. Zhang SY, Gao F, Peng CG, Zheng CJ, Wu MF. miR-485-5p promotes osteoporosis via targeting Osterix. *Eur. Rev. Med. Pharmacol. Sci.* 2018; 22(15):4792-4799. doi:10.26355/eur-rev\_201808\_15613
40. Lu XD, Han WX, Liu YX. Suppression of miR-451a accelerates osteogenic differentiation and inhibits bone loss via Bmp6 signaling during osteoporosis. *Biomed. Pharmacother.* 2019; 120:109378. doi:10.1016/j.biopha.2019.109378
41. de Vasconcellos JF, Jackson WM, Dimtchev A, Nesti LJ. A microRNA Signature for Impaired Wound-Healing and Ectopic Bone Formation in Humans. *J. Bone Joint Surg. Am.* 2020; 102(21):1891-1899. doi:10.2106/jbjs.19.00896
42. Gong Y, Yuan S, Sun J, et al. R-Spondin 2 Induces Odontogenic Differentiation of Dental Pulp Stem/Progenitor Cells via Regulation of Wnt/ $\beta$ -Catenin Signaling. *Front Physiol.* 2020; 11:918. doi:10.3389/fphys.2020.00918
43. Yang S, Guo S, Tong S, Sun X. Exosomal miR-130a-3p regulates osteogenic differentiation of Human Adipose-Derived stem cells through mediating SIRT7/Wnt/ $\beta$ -catenin axis. *Cell Prolif.* 2020; 53(10):e12890. doi:10.1111/cpr.12890
44. Cui Y, Luan J, Li H, Zhou X, Han J. Exosomes derived from mineralizing osteoblasts promote ST2 cell osteogenic differentiation by alteration of microRNA expression. *FEBS Lett.* 2016; 590(1):185-192. doi:10.1002/1873-3468.12024
45. Xu Q, Cui Y, Luan J, Zhou X, Li H, Han J. Exosomes from C2C12 myoblasts enhance osteogenic differentiation of MC3T3-E1 pre-osteoblasts by delivering miR-27a-3p. *Biochem. Biophys. Res. Commun.* 2018; 498(1):32-37. doi:10.1016/j.bbrc.2018.02.144
46. Huang Y, Xu Y, Feng S, He P, Sheng B, Ni J. miR-19b enhances osteogenic differentiation of mesenchymal stem cells and promotes fracture healing through the WWP1/Smurf2-mediated KLF5/ $\beta$ -catenin signaling pathway. *Exp. Mol. Med.* 2021. doi:10.1038/s12276-021-00631-w